Downloaded from http://rsfs.royalsocietypublishing.org/ on December 31, 2014

Interface Focus

rsfs.royalsocietypublishing.org

Review

Cite this article: Sturm JC, Cox EC, Comella B, Austin RH. 2014 Ratchets in hydrodynamic flow: more than waterwheels. *Interface Focus* **4**: 20140054.
http://dx.doi.org/10.1098/rsfs.2014.0054

One contribution of 13 to a Theme Issue 'Biophysics of active systems: a themed issue dedicated to the memory of Tom Duke'.

Subject Areas:
biophysics, biotechnology

Keywords:
microfluidic arrays, ratchets, hydrodynamic flow

Author for correspondence:
Robert H. Austin
e-mail: austin@princeton.edu

Ratchets in hydrodynamic flow: more than waterwheels

James C. Sturm[1], Edward C. Cox[2], Brandon Comella[4] and Robert H. Austin[3]

[1]Department of Electrical Engineering, [2]Department of Molecular Biology, and [3]Department of Physics, Princeton University, Princeton, NJ 08544, USA
[4]Department of Physics, California Institute of Technology, Pasadena, CA 91125, USA

The transport of objects in microfluidic arrays of obstacles is a surprisingly rich area of physics and statistical mechanics. Tom Duke's mastery of these areas had a major impact in the development of biotechnology which uses these ideas at an increasing scale. We first review how biological objects are transported in fluids at low Reynolds numbers, including a discussion of electrophoresis, then concentrate on the separation of objects in asymmetric arrays, sometimes called Brownian ratchets when diffusional symmetry is broken by the structures. We move beyond this to what are called deterministic arrays where non-hydrodynamic forces in asymmetric arrays allow for extraordinary separation, and we look to the future of using these unusual arrays at the nanoscale and at the hundreds of micrometre scale. The emphasis is on how the original ideas of Tom Duke drove this work forward.

1. Introduction

It is not often that a pure theorist such as Tom Duke is able to make a real impact on biotechnology. Usually biotechnology is developed by the experimentalist, with perhaps the theorist helping out in analysis of the data. In the case of Tom's work, the effort was truly collaborative, and in fact we were often following and Tom was leading. Also fortunately for us, Tom did not belong in the 'resist new ideas at all costs' camp that sometimes afflicts science. We *think* that one of the first examples of using microfabrication for the analysis of biological molecules came from our early attempt to fractionate DNA by length in a synthetic 'gel' microfabricated out of silicon posts, carried out at Cornell's pioneering Cornell Nanofabrication Facility [1]. About this time, we were invited to a workshop on the island of Cargese and presented this work, including the puzzling fact that the DNA in the post array was extremely elongated even at very low electrophoretic speeds of micrometres per second. Tom of course was a student of Sam Edwards at Cambridge and knew a great deal about polymer dynamics from a theoretical perspective, and we knew very little. Tom's education of electrophoresis was greatly advanced by his work with Viovy [2,3] in several pioneering papers. Somehow we managed to obtain support for Tom to spend a postdoctoral period at Princeton (a great lucky break) as we worked together on the dynamics of DNA in microfabricated environments. Understanding the dynamics of long double-strand DNA molecules in synthetic arrays turned into a gateway project for much that came later.

2. Some really basic physics about charged polymers we had to learn from Tom

Ultimately, we failed to separate DNA in the post array [4], for a couple of very simple but somewhat deep physics reasons that we learned from Tom, who was a master of the subject. We suppose if we had known Tom earlier before we made the array perhaps we would have been discouraged from trying it, so perhaps it is a good thing that we first made an initial scientific *faux pas*. Let us recite the two main mistakes.

© 2014 The Author(s) Published by the Royal Society. All rights reserved.

Royal Society Publishing

Downloaded from http://rsfs.royalsocietypublishing.org/ on December 31, 2014

2.1. Charged polymers in saline solution do not show a net charge at large distances

That is, the oppositely charged mobile ions in solution around the polymer neutralize the polymer as they are attracted to the polymer, so beyond a characteristic distance, called the Debye length, the polymer is effectively neutral. This is a well-known fact, but people keep forgetting it. The Debye length is usually given by the exponential spatial rate κ by which the local charge on the polymer is neutralized.

The buffer used in a saline solution essentially creates a plasma of positive and negatively charged ions in the water. When you apply a potential difference across the solution, positive ions are transported towards the cathode and negative ions are transported towards the anode. Now consider a highly charged molecule such as DNA in solution. The negative charges of the phosphate backbone will attract a cloud of positive ions and repel the negative ions. A simple (non-rigorous) description of the density of ions at a distance r from a point charge can be found in the textbook by Jackson [5]. Poisson's equation states that the electrostatic potential Ψ must satisfy the following equation:

$$\nabla^2 \Psi = n(r), \tag{2.1}$$

where $n(r)$ is the charge density at a distance r. We can recast the equation solely in terms of the potential Ψ by noting that the spatial distribution must obey the Boltzmann factor

$$n(r) = n_o \exp\left(\frac{-e\Psi}{k_B T}\right), \tag{2.2}$$

where n_o is the bulk equilibrium ion concentration. We thus get the following (horrendous) equation:

$$\nabla^2 \Psi = -4\pi e\delta(r) - 4\pi e n_o \left[\exp\left(\frac{-e\Psi}{k_B T}\right) - 1\right]. \tag{2.3}$$

As a simple first-order approximation, we can linearize this equation for $(e\Psi/k_B T)$ small

$$\nabla^2 \Psi - \frac{4\pi n_o e^2}{k_B T} \sim -4\pi e\delta(r) + 4\pi e\epsilon_o n_o \frac{e\Psi}{k_B T}, \tag{2.4}$$

which has the following solution:

$$\Psi(r) = \frac{e\exp(-r/\kappa_D)}{r}, \tag{2.5}$$

where κ_D is the Debye screening length

$$\kappa_D = \left[\frac{k_B T}{4\pi n_o e^2}\right]^{1/2}. \tag{2.6}$$

Note that this number can be surprisingly small. Let us assume that we have a 100 mM solution of NaCl at 300 K. The Debye screening length is about 1 Å! Thus, the counter-ions shield the naked charge of the DNA quite effectively. In the case of a linear molecule like DNA, the situation is more complicated and a 'condensation' of charge occurs which results in a more or less constant shielding of the charged backbone from 1 mM to 0.5 M in salt [6].

Now, consider what happens when the polymer moves in response to an applied external field. As the charged backbone of the polymer moves in one direction, the oppositely charged counter-ions move in the opposite direction, and they are closely coupled to the surface of the polymer.

There is a fundamental difference between the dynamics of polymers in pure hydrodynamic flow and in electrophoresis. The hydrodynamic interaction between two objects in solution is the result of the Oseen–Burgers tensor that couples them via hydrodynamics. The velocity flow field $\mathbf{u}(r)$ at right angle to a sphere of radius a moving with velocity $\mathbf{U}$ is

$$\mathbf{u}\left(\theta = \frac{\pi}{2}\right) = \frac{\mathbf{U}}{r}\left[\frac{3a}{4} + \frac{a^3}{4r^2}\right]. \tag{2.7}$$

Note the expected $1/r$ decrease in the velocity with radius. This gives rise to all sorts of troubles and is in fact incorrect at 'large' distances from the sphere. The problem is that our assumption that the inertial terms in the Navier–Stokes equation are always small is incorrect, surprisingly. Lifshitz & Pitaevskii [7] or Batchelor [8] give an intuitive understanding of why this is true.

To first order, the velocity as a function of large distance falls off as $3Ua/4r$ from equation (2.7), and hence the gradient in the velocity falls off as roughly $-Ua/r^2$. Hence, the inertial terms in equation (4.1) which have the form $(u\cdot\nabla)u$ will scale as $\rho U^2 a/r^2$. However, the viscous term $\eta\nabla^2 U$ scales as $\eta\ Ua/r^3$ and hence falls off much more rapidly than the inertial term. Thus, the effective R_e of the flow field increases with increasing distance from the polymer and becomes of order 1 at a distance given by

$$R_{\text{crit}} \sim \frac{\eta}{U\rho}, \tag{2.8}$$

which interestingly is independent of the size of the object! For typical velocities U of 10 μm s^{-1} we find that $R_{\text{crit}} \sim 1$ cm, a rather huge distance. The lesson here seems to be for low R_e flow that laminar flow patterns effectively reach out to infinity, and hence that DNA will most certainly be a non-free draining polymer under pure hydrodynamic flow fields. DNA molecules can be separated by length using pure hydrodynamic flow.

But all this fails in electrophoresis! The Debye screening length sets a scale beyond which mobile ions do not interact electrostatically with the charged polymer, and further it sets a shear boundary between the ions and the DNA. That is, within the Debye length, the counter-ions, which normally would be moving in a direction opposite to the motion of the charged polymer in an applied field, co-move with the polymer, and there is no viscous dissipation. Beyond the Debye length, the counter-ions can move opposite to the polymer movement, and this sets up a hydrodynamic shear boundary and viscous dissipation. Unfortunately, under conditions where dsDNA is stable (10 mM salt), the Debye length is much smaller than the radius of gyration of a long dsDNA molecule and the polymer is said to be 'free-draining': the electrophoretic mobility is independent of the length of the dsDNA [9], which means that you cannot separate long DNA molecules as a function of length in free solution.

This is why gels were developed, to bring in higher order length-dependent drag coefficients, and why we built the post array. But this too fails if the polymer becomes elongated, and it does so easily. In what follows, although we will talk about electric fields E in the fluid, the reader should be reminded that we are really talking about the hydrodynamic drag/length that is exerted on an object due to the movement of ions in the fluid at the hydrodynamic shear boundary layer.

Downloaded from http://rsfs.royalsocietypublishing.org/ on December 31, 2014

2.2. Long polymers form very soft globules which have very low effective bulk moduli and are very easily deformed

What is wrong is our assumption that the coil statistics are really Gaussian: in the presence of a field, there is a tendency for the head of the polymer to become 'biased' in its walk, hence the origin of the term 'biased reptation model' [10]. Some simple considerations can reveal the basic polymer physics of the model. We will assume that the gel pores are of the order of a persistence length, so that the only free section as the polymer moves forward is basically one persistence length of the molecule. The 'polarization' or orientation of the leading section is easy to calculate and is the same as similar considerations in dielectric polarization and paramagnetism. Let us assume that the effective pore size is a, and that it is about equal to the persistence length p. The Boltzmann relation then can be used to calculate the average value of $\cos\theta$, where θ is the angle between the tangent of the free end of the polymer jutting into the pore and the electric field

$$\langle \cos(\theta)\rangle = \frac{\int \cos(\theta)\sin(\theta)\exp(-a^2\lambda E/k_BT)}{\int \sin(\theta)\exp(-a^2\lambda E/k_BT)}, \tag{2.9}$$

which is the Langevin function $L(E^*)$

$$\langle \cos(\theta)\rangle = L(E^*) = \coth(E^*) - \frac{1}{(E^*)}, \tag{2.10}$$

where it is convenient to define the dimensionless electric field E^*

$$E^* = \frac{\lambda a^2 E}{k_BT}. \tag{2.11}$$

Note that E^* is a measure of the orientation of the polymer head, and that as E^* gets large, the orientation can in principle get large and hence the DNA becomes highly elongated. And it does.

The polymer dynamics we learned from Tom was used by graduate student Olgica Bakajin and post-docs Chia-Fou Chou, Christelle Prinz, Jonas Tegenfeldt, Han Cao and Robert Riehn, and later graduate student Walter Reisner to develop some very powerful ideas to align DNA in true nanochannels [11–15]. This technology is growing strong, and the company BioNanogenomics (http://www.bionanogenomics.com/) is now actively marketing a device for mapping genomic length DNA molecules which combines the post array and nanochannels, and it all maps back to Tom and his work with us as experimentalists.

3. Maxwell's demon and Tom Duke: the diffusion array

It is a mark of true originality that some ideas come completely out of left-field, as Americans familiar with baseball say. We would not go through all the travails Tom went through in trying to figure out how to separate long DNA molecules given they elongate so easily, but rather refer you to the literature [16,17]. Basically, there are work-arounds to the elongation problem that Tom came up with that fully used rather than fought elongation, but it was a struggle.

However, Tom came up with an idea that originated with the earlier pioneering work of Ajdari & Prost [18]: why not use broken symmetry to separate molecules (such as DNA, but it could be anything) based on their diffusion constant and some clever structures based upon the ability of microfabrication to make rather 'unnatural things' [19]. 'Broken symmetry' is one of those fundamental ideas that physicists like but profoundly irritates engineers because it seems to take a simple idea and make it sound mysterious, but sometimes there really is depth in the idea. Up to the point that Tom came up with this insight following his work with Prost, all our arrays had been symmetrical in a mirror reflection (which changes $+z$ to $-z$, but leaves x and y unchanged). Tom effectively suggested: why not turn your round posts into rectangles and rotate the rectangles an angle $\Delta\theta$ around $\hat{y}$-axis as shown in figure 1. While Tom was not the first to suggest the impact of broken symmetry [20], in the words of one of the referees, it was 'Tom's combination of knowledge in polymers, electrophoresis and ratchets (among all the other stuff he knew about) that made him the person for the job'.

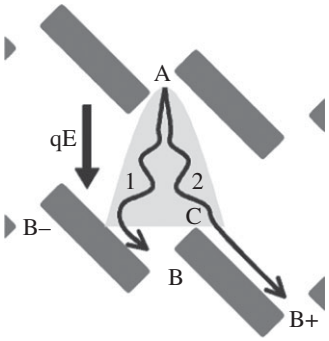

Figure 1. A scanning electron micrograph of a rotated array designed by Tom Duke. Transverse Brownian motion may cause a molecule to skip one channel to the right if it diffuses through displacement, or very rarely, one channel to the left.

The brilliance behind this idea was that it effectively rectified Brownian motion in the presence of laminar flow due to the asymmetry of the rotated rectangles. Objects that diffused a distance further than a critical distance δ_r to the right would be deflected over to the next column of open channels, while objects that diffused the distance δ_t would simply be refocused back to the same channel. The device worked, but not with high precision, because the device only took a cut on the total number of molecules moving to the right.

More exactly, the probability $P(x,y)$ for a particle with diffusion constant D moving with advective speed v in the y-direction to diffuse a distance x is given by

$$P(x,y) = \left[\frac{v}{4\pi Dy}\right]^{1/2} \exp\left[-\frac{x^2 v}{4Dy}\right]. \tag{3.1}$$

The 'cut' $p(x_{split}, y)$ this device makes is then made in the probability distribution if the effective splitting distance is x_{split}

$$p(x_{split}, y) = \int_{x_{split}}^{\infty} P(x,y)\mathrm{d}x. \tag{3.2}$$

Unfortunately for this device, one has to move the object rather slowly to try and optimize $p(x_{split}, y)$, and the cut is in any event rather small.

4. The bump array: taking advantage of mistake

But the basic idea of broken symmetry and rectified motion had been planted by Tom. It remained for a brilliant graduate

Downloaded from http://rsfs.royalsocietypublishing.org/ on December 31, 2014

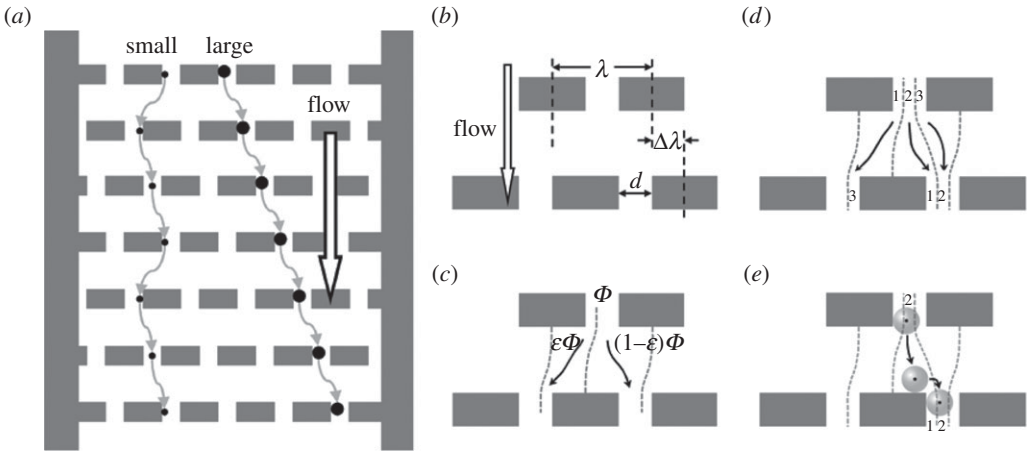

Figure 2. (*a*) Basic structure of a microfluidic channel filled with obstacles, where small particles migrate in the zig-zag mode and large particles in the bump mode. (*b*) Geometric parameters defining the obstacle matrix. (*c*) Bifurcation of fluid flows in the obstacle matrix. Dashed curves represent stagnant streamlines dividing the bifurcating flow. (*d*) Fluids from different relative positions (slots) flow to different slots in a predictable manner: slot 1 → slot 3 → slot 2 → slot 1. (*e*) Large particles are physically displaced by obstacles. The dots on the spheres represent the hydrodynamic centres-of-mass, which always fall in slot 2.

student, Richard Huang, to make the unexpected leap to using the unusual behaviour of flow at low Reynolds number R_e to get rid of diffusion altogether and simply let broken symmetry work.

But we discovered it by mistake. Richard Huang understood that for Tom's Brownian ratchet to work, the flow lines had to be accurately down the axis of the array, and because of the broken symmetry this was not so easy to do unless one paid very close attention to the boundary conditions of the flow entering the device. Richard worked very hard at solving this problem along with student Nick Darnton [21], but on one magic day because of some blocked injection channels Richard had flow lines moving at an angle ϵ to the clear axis of a tilted array: to his astonishment, the separation seemed to be enhanced rather than destroyed by wrong flow conditions!

Fortunately for us, instead of immediately fixing the problem Richard Huang realized something none of us, not even Tom, had realized: that it was possible to achieve deterministic separation of objects based on their radius without using diffusion [22]. The idea is actually rather subtle, because the equations of motion that govern laminar flow in all these devices would seem to be symmetric with time and direction in the absence of diffusion.

The basic equation governing incompressible fluid dynamics is the Navier–Stokes equation, usually written as

$$-\nabla P + \eta\nabla^2\boldsymbol{u} = \rho\left(\frac{\partial u}{\partial t} + (\boldsymbol{u}\cdot\nabla)\boldsymbol{u}\right). \tag{4.1}$$

This is just Newton's law of motion for fluids, $\boldsymbol{F} = \mathrm{d}\boldsymbol{P}/\mathrm{d}t$: the left-hand side represents the forces acting on a voxel of water, and the right-hand side represents the total change in momentum of the voxel with time. The above equation can be viewed as saying that the forces per unit volume due to a pressure gradient, ∇P, and viscosity, $(\eta\nabla^2\boldsymbol{u})$, are equal to the mass per unit volume, ρ, times the acceleration of the fluid. The right-hand side terms are sometimes referred to as the 'inertial forces', although they are not forces in the strict physics use of the word. If there are additional forces acting on the fluid (for instance, gravity), these terms are just added onto the left-hand side (ρg). The two terms on the right are just the total derivative of the velocity $\mathrm{d}\boldsymbol{u}/\mathrm{d}t$ rewritten in terms of partial derivatives for vectors.

At low R_e, like these, the Navier–Stokes equation is particularly simple, as we can effectively ignore the right-hand side of equation (4.1). This transforms a nonlinear partial differential equation into a simple linear one. The fluid flow is determined entirely by the pressure distribution and, of course, the boundary conditions ($v = 0$ at the walls). This type of flow is known by various names: 'Stokes flow', 'creeping flow' or most simply and clearly 'low Reynolds number flow'. The governing equation is

$$\eta\nabla^2\boldsymbol{u} = \nabla P, \tag{4.2}$$

which is known as Laplace's equation, a well-studied differential equation in mathematical physics.

Note that equation (4.2) contains no time derivatives unlike the Navier–Stokes equation (4.1). Because of this, under low Reynolds number conditions, *all motion is symmetric in time*, meaning that if the pressures or forces exerted on the fluid are reversed, the motion in the fluid is completely reversed [23].

How then could Richard have obtained separation moving larger objects to the right if the flow lines are reversible? The answer is that when an object touches a wall, there are added non-hydrodynamic terms in the equation of motion, and these terms break symmetry. In what we came to call the 'bump array', the touching of an object with the array posts pushes the object off to one side: this is a new force and if the object is big enough can push it into an adjacent flow pattern. Figure 2 shows the basic idea.

It is amusing to note that when this idea was in press in *Science* the Editor took it upon himself to make 'corrections' to the text and changed the title from the correct but we guess too flip 'A Microfluidic Tango: Separation Without Dispersion' to the totally stiff-necked and incorrect 'Continuous Particle Separation through Lateral Dispersion'. Noooo! He missed the point. The point is that this device separates objects deterministically. The crucial number here is the Peclet number P_e, which is defined as the ratio of the time t_D to diffuse a distance x to the time t_A to advect a distance x if the particle is being transported at a speed v

$$P_e = \frac{t_\mathrm{D}}{t_\mathrm{A}} = \frac{x^2}{2D}\times\frac{v}{x} = \frac{xv}{2D}. \tag{4.3}$$

As long as $P_e > 1$, the bump array is very good in sorting particles by size deterministically.

Downloaded from http://rsfs.royalsocietypublishing.org/ on December 31, 2014

The bump-array concept of deterministic separation of particles without diffusion is powerful because of the advantages it offers:

(1) It works well at high P_e; in fact for rigid objects the higher the Peclet number the better you are, unlike a Brownian ratchet where the performance degrades with P_e.
(2) It can be made non-clogging, by simply arranging for larger particles to be bumped out first, then decreasing the characteristic spacing d between the tilted array posts. This is called a 'chirped' array.
(3) It can run through large volumes of fluid, as one simply has to increase P_e, and still find a very few outlier particles.

5. Real ratchets via broken symmetry

It is possible to design a true microfluidic ratchet where the trajectories of particles in a certain size range are not reversed when the sign of the driving force is reversed, as a student, Kevin Loutherback, discovered. First, we point out again that because of the non-hydrodynamic forces exerted by particles when they touch a wall we should not expect the basic symmetry of the Navier–Stokes equation at low R_e, equation (4.2), to be obeyed in any event. Figure 3, taken from Dr Loutherback's thesis (https://www.princeton.edu/~sturmlab/theses/klouther_thesis.pdf), makes this clear that reversing paths does not get you to the same initial starting point. But this is a one-step ratchet; once displaced vertically the sphere does not undergo any further displacements.

But a true ratcheting effect, that is, transverse particle one-way motion without any net fluid flow, can be produced by employing right isosceles triangles rather than the conventional circular posts in a tilted post array. A right triangle now breaks the symmetry even further. Thus, using broken symmetry with right-triangle posts particles can be separated without any net motion of the fluid. The underlying mechanism of this method is due to an asymmetric fluid velocity distribution through the gap between posts because of the broken symmetry of the right triangle. This can be seen in figure 4, which compares using simulations of the fluid flows for the cylinder and right-triangle cases.

Because of the symmetry of the Navier–Stokes equation (4.1), you might think that reversing the path of the particles is the same as simply rotating the array 180°: the flows are reversible in time. But not the particle motions! We observed that particles in an intermediate size range in a bump array with triangular posts did not retrace their trajectory when the fluid was reversed. Rather, they seemed to switch between behaving like small particles which follow the fluid flow axis to behaving like large particles that follow the tilted array axis when the direction of the fluid flow was reversed. As a result, cycling the fluid motion back and forth produced a net displacement perpendicular to the fluid flow axis as intermediate particles ratcheted up the array. The path is not reversed when the fluid flow direction is reversed, with the net result that such particles are separated from their original position in a perpendicular direction to the oscillatory flow [24]. Observed over many cycles, intermediate-sized particles were concentrated along one edge of the device and could not be returned to their original positions.

Small particles, which are not displaced by the posts, do not show any net displacement as the fluid is cycled back and forth. Figure 5*a* shows the trajectory of a 1.1 μm diameter bead in the array. As the particle moves forward, it takes many small steps parallel to the array axis as it moves through, followed by one larger step perpendicular to the motion of the fluid (in what we refer to as 'zig-zag mode'), so that the net motion is in the same direction as the bulk fluid. When the direction of the fluid is reversed, it retraces its trajectory and returns to its original position.

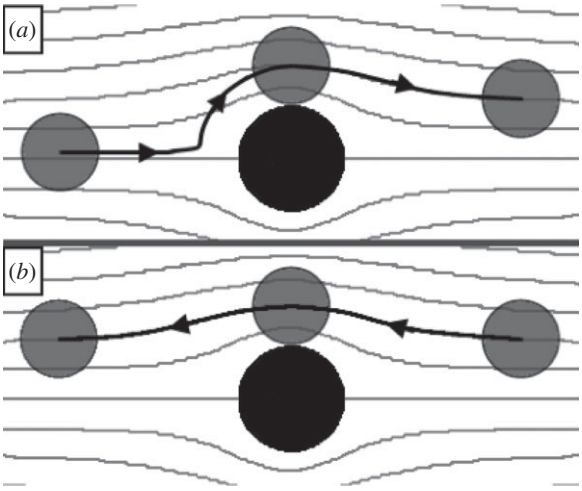

Figure 3. Irreversible particle motion results when a particle runs into an obstacle. (*a*) A particle moving left to right is displaced to a new streamline when it runs into a post. (*b*) When the flow is reversed, the particle follows its new streamline and returns to a different initial position.

Figure 5 shows a broken-symmetry array which was microfabricated to test these ideas. This array features right isosceles triangular posts with 6 μm length, a gap between posts of approximately 4 μm and 1/10 array tilt. The array was fabricated in silicon by reactive-ion etching to a depth of approximately 10 μm.

Large particles, which are displaced by the posts, also do not show any net displacement when the fluid is cycled back and forth. Because the particles are displaced from its flow path by the posts in each column, we refer to this as 'bumping mode'. When the direction of the fluid is reversed, it retraces its trajectory and returns to its original position. Intermediate particles follow a hybrid trajectory that is a combination of the previous two paths. Figure 5*c* shows the trajectory of a 1.9 μm diameter bead in the array. This particle 'zig-zags' like a small particle when going to the right to follow the fluid flow but 'bumps' like a large particle when going to the left to follow the post array axis. Its path is not reversed when the fluid flow direction is reversed, with the net result that such particles are separated from their original position in a perpendicular direction to the oscillatory flow. Observed over many cycles, intermediate-sized particles were concentrated along one edge of the device and could not be returned to their original positions.

Tom started by thinking about true ratchets; unfortunately it took us about 20 years to truly realize the phenomena, and even then through the ideas of Kevin Loutherback.

6. Moving towards the very big and the very small: Tom marches on

The work that Tom started is moving on, to the very big, and the very small. Both of the present projects are directed towards fundamental issues in cancer. Without Tom's pushing on the initial Brownian ratchet, none of this would have happened.

Downloaded from http://rsfs.royalsocietypublishing.org/ on December 31, 2014

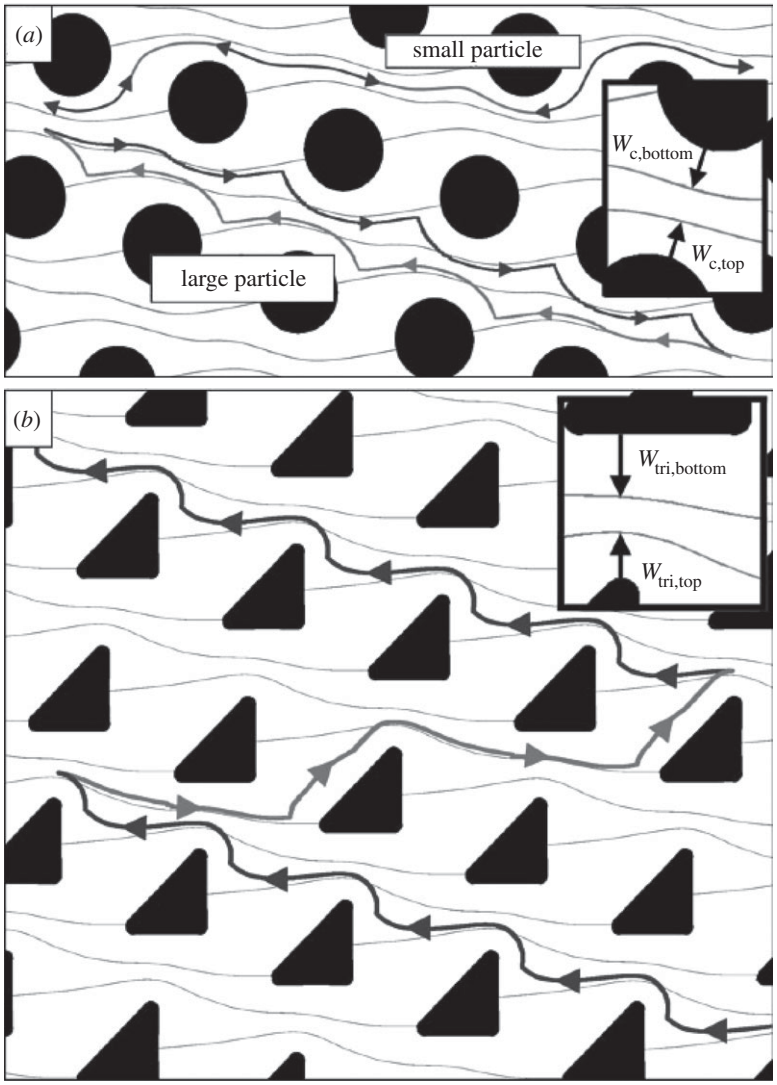

Figure 4. Simulated particle trajectories in DLD arrays with ϵ of 1/3 in oscillating flow for (*a*) round and (*b*) right triangular posts. Insets indicate the widths of the streams in the gap adjacent to the posts in both cases. (*a*) Paths of small and large particles moving both left to right and right to left, both of which macroscopically retrace their paths. (*b*) Path of a ratcheting particle in an array with right triangular posts, where the particle acts as a large particle travelling right to left but as a small particle when travelling left to right.

6.1. The very big

The very big scale concerns cells (or groups of cells) that move from local tumours to remote sites in the body, the final deadly end-game in cancer called metastasis that is responsible for about 90% of cancer deaths. There is a large effort at present to find and detect these cancer cells as they move from the tumour to the distant sites, in the desperate hope that (i) if we can intercept them we can prevent metastasis or (ii) the more immediate hope is that we can detect them and determine what kind of cancer they represent and develop a treatment for that particular cancer before it has spread. It is a great idea, but there are four basic problems in the quest for these circulating tumour cells (CTCs) [25].

(1) They seem to be very rare, approximately 1–100 ml^{-1} of whole blood. As a millilitre of blood contains about 10^9 red blood cells and about 10^6 white blood cells (basically immune system cells with nuclei, unlike the red blood cells which except in special cases have no nuclei). This means that one is looking for of the order of 1 cell out of 100 million cells in the worst case scenario.

(2) Although CTCs have nuclei and as they are about 30 μm in diameter are easily sorted from the abundant but smaller red blood cells, they are not believed to be much larger than white blood cells. The numbers are not well known, but one can guess that the 'average' white blood cell is about 20 μm in diameter, and a 'typical' CTC is of the order of 30 μm in diameter. So, of the 1 million cells with nuclei in a millilitre of whole blood, you need to separate out about 100 of them which are believed to be CTCs, and these 100 cells are only about 10 μm bigger than the average size.

(3) The average 'efficiency' of a CTC to form a tumour seems to be very low; of course this is just an educated guess, but the estimates are that only about 10^{-4} of the CTCs actually go on to form remote tumours.

(4) The low efficiency leads to the guess that there would not be a great correlation between the number of CTCs found using the various immunological methods presently used for finding CTCs in blood and the presence of metastatic cancers. In fact, CTC count would seem to be a poor indicator of metastatic potential.

All of these issues should discourage one from looking for CTCs as indicators of metastasis, except for one possibility: perhaps what we should be looking for are not *isolated* CTCs, but rather very rare *clumps* of cells, which contain both tumour cells and the so-called stromal cells that are

Downloaded from http://rsfs.royalsocietypublishing.org/ on December 31, 2014

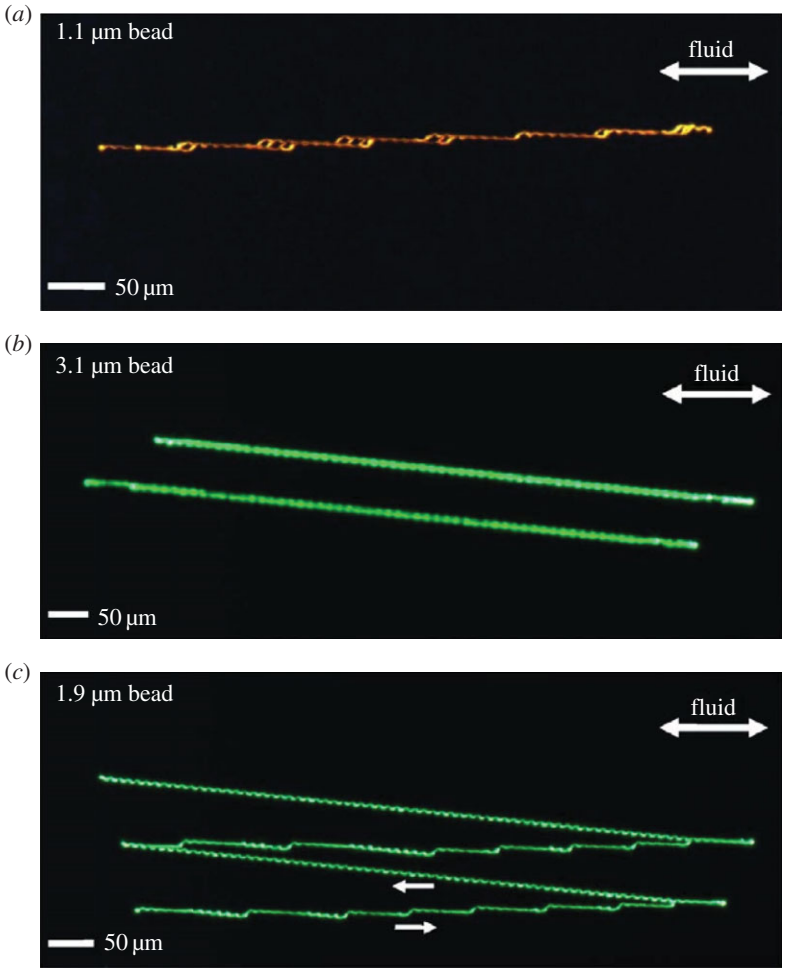

Figure 5. Images of trajectories of spherical polystyrene beads of three different sizes in a right-triangle array as the direction of fluid flow is cycled back and forth twice. Particle sizes are (*a*) 1.1, (*b*) 3.1 and (*c*) 1.9 μm. Particles in (*a*,*b*) retrace their paths when the direction of the fluid is switched while the trajectory in (*c*) varies with the direction of the fluid flow. In (*c*), small arrows indicate the direction of the fluid along the particle path. (Online version in colour.)

known to be needed for many cancers to grow [26]. That is, while isolated CTCs have a very low efficiency for generation of metastatic lesions, it is possible that larger clumps of tumour cells with support cells would have a far greater efficiency, but right now most efforts are focused on single CTCs rather than rarer, larger clumps.

In order to see rare, large clumps, it is necessary to scale up the bump arrays, and it is necessary to make the 'de-watering' of the device as great as possible. By 'de-watering', we mean the concentration of the selected objects as great as possible, and still maintain high flow rates. These things add up to a *big* array, in fact a 300 mm array.

The basic reasons for such a large array are the need for close to a thousand channels spaced several hundred micrometres apart. The bump array can do no better than bump N channels into one channel, even though the flow is deterministic and precise. Thus, if one is looking for rare objects, one needs as many channels as possible. Given that we are looking for large clumps, and thus channels that are several hundred micrometres across, a concentration of $1000\,l^{-1}$ requires an array that is 200 mm across. Of course, this also helps the flow rate, because the flow for a fixed pressure gradient will scale as the number of channels. Unfortunately in US academia, there are no 300 mm wafer processing facilities, in spite of the fact that in industry modern fabrication foundries have long since moved to 400 mm wafers, and larger. At Princeton, we have been forced to develop our own 300 mm wafer processing equipment without spending a fortune, but

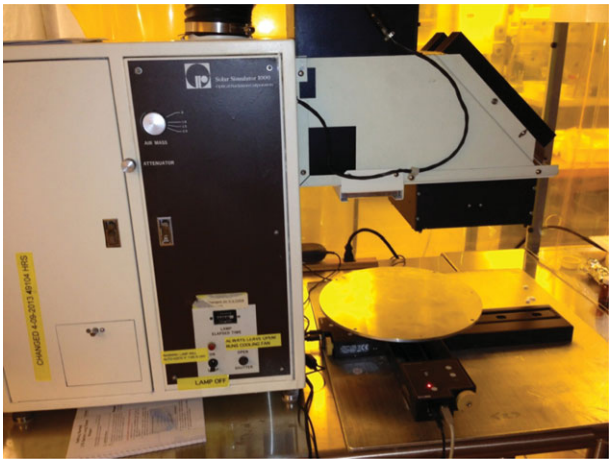

Figure 6. Stage. (Online version in colour.)

it has been difficult. Figure 6 shows the motorized stage that moves 300 mm wafers over the 200 mm light source in such a way as to optimize uniform illumination during the exposure. Figure 7 shows a 300 mm wafer that has been exposed and developed. At present, we are testing out the performance of the device.

6.2. The very small

At the other end of the size spectrum is the sub-micrometre world of objects that flow in the blood, about which we

Downloaded from http://rsfs.royalsocietypublishing.org/ on December 31, 2014

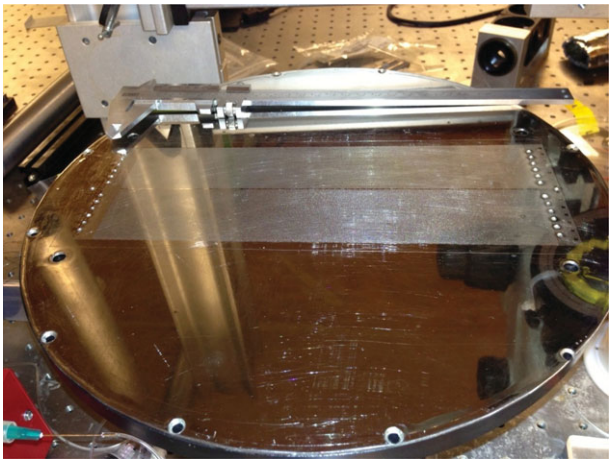

Figure 7. Wafer. (Online version in colour.)

really know very little because of the difficulty of seeing them, especially if their characteristic size is less than the wavelength of visible light. The problem is doubly compounded if the sub-micrometre objects are rare. It has become clear, however, that there are sub-micrometre circulating particles in the blood and that they are biologically important. For the purpose of this article, we will concentrate on the objects known as exosomes [27]. Exosomes are small (50–100 nm) vesicles that are secreted by a large variety of cells in the body and travel around the bloodstream. Exosomes are connected with a great many signalling events in biology and neurobiology, the neurobiology connection being particularly interesting because the exosomes can apparently penetrate the blood–brain barrier. Because of this easy penetration, they may be closely involved with tumour spreading and the process of metastasis. Unlike the 'seeds and soil' aspect that we discussed above, where you try to find the actual functional cells that are spreading the tumour, in the case of exosomes one is looking for the signals and contents of the exosomes that are being spread.

There are several difficulties at present in characterizing the exosomes in the blood. For example, they certainly are not of a uniform size: there is believed to be a distribution of sizes from 50 to 100 nm. It is not really known what is the number density of the exosomes in a normal, healthy person's blood. A further complication is that at least in whole blood there are numerous 'contaminates' that are not exosomes but are of a similar size. However, in filtered bodily fluids, it is expected that the exosome purity will be substantially higher [28].

Although we have worked a great deal with Tom's technology of ratcheting Brownian motion and the subsequent offspring such as the deterministic bump array, we have never pushed down into the sub-micrometre scale. Here, the Peclet number becomes quite important. We can do a simple calculation to estimate the needed flow rates in a bump array to separate out 100 nm objects. The scale of the distance L between the posts will have to be of the order of 1 μm, and if we want the bump array to work we will not want the object to diffuse a distance greater than about $x = L/10$ or about 100 nm. The diffusion coefficient D of a sphere of radius R in a fluid of viscosity η is

$$D = \frac{k_B T}{6\pi\eta R}. \tag{6.1}$$

It takes around 10^{-3} s for such an object to diffuse 100 nm, so the minimum flow speed assuming 1 μm between the successive posts is of the order of 10^3 μm s^{-1}, a fairly high speed but by no means out of reach. We are pushing now into regions where no one has made such ratcheting structures. At this point, we have nanofabricated at Cornell a deterministic bump array using the ASML 300C DUV Stepper which is capable of reaching scales down to 100 nm. Even smaller features are possible using e-beam large array technologies, which are out of reach for academia. However, we have begun a collaboration with IBM Research Labs and hope to combine the theoretical insights of Tom Duke which started all this biotechnology with the large-scale processing powers and experimental expertize they have to fully realize some of the dreams that Tom had.

Acknowledgements. The content is solely the responsibility of the authors and does not necessarily represent the official views of the National Cancer Institute, the National Institutes of Health or the National Science Foundation.

Funding statement. This work was performed in part at the Cornell NanoScale Facility supported by the National Science Foundation (grant no. ECS 03-35765). The research described was supported by an award (U54CA143803) from the US National Cancer Institute and in part by the National Science Foundation under grant no. PHYS-1066293 of the Aspen Center for Physics.

References

1. Volkmuth WD, Austin RH. 1992 DNA electrophoresis in microlithographic arrays. *Nature* **358**, 600–602. (doi:10.1038/358600a0)
2. Viovy JL, Duke T, Caron F. 1992 The physics of DNA electrophoresis. *Contemp. Phys.* **33**, 25–40. (doi:10.1080/00107519208219138)
3. Duke TAJ, Semenov AN, Viovy JL. 1992 Mobility of a reptating polymer. *Phys. Rev. Lett.* **69**, 3260–3263. (doi:10.1103/PhysRevLett.69.3260)
4. Volkmuth WD, Duke T, Wu MC, Austin RH, Szabo A. 1994 DNA electrodiffusion in a 2D array of posts. *Phys. Rev. Lett.* **72**, 2117–2120. (doi:10.1103/PhysRevLett.72.2117)
5. Jackson JD. 1999 *Classical electrodynamics*, 3rd edn. New York, NY: Wiley. (http://cdsweb.cern.ch/record/490457).
6. Manning GS. 2002 Electrostatic free energy of the DNA double helix in counterion condensation theory. *Biophys. Chem.* **101**, 461–473. (doi:10.1016/S0301-4622(02)00162-X)
7. Lifshitz EM, Pitaevskii LP. 2002 *Statistical physics. Part 2. Theory of the condensed state*. Oxford, UK: Butterworth-Heinemann.
8. Batchelor G. 2000 *An introduction to fluid dynamics*. Cambridge Mathematical Library. Cambridge, UK: Cambridge University Press. (http://books.google.com/books?id=Rla7OihRvUgC).
9. Meagher RJ, Won JI, McCormick LC, Nedelcu S, Bertrand MM, Bertram JL, Drouin G, Barron AE, Slater GW. 2005 End-labeled free-solution electrophoresis of DNA. *Electrophoresis* **26**, 331–350. (doi:10.1002/elps.200410219)
10. Viovy JL, Duke T. 1993 DNA electrophoresis in polymer solutions: Ogston sieving, reptation and constraint release. *Electrophoresis* **14**, 322–329. (doi:10.1002/elps.1150140155)
11. Tegenfeldt JO *et al*. 2001 Near-field scanner for moving molecules. *Phys. Rev. Lett.* **86**, 1378–1381. (doi:10.1103/PhysRevLett.86.1378)
12. Prinz C, Tegenfeldt JO, Austin RH, Cox EC, Sturm JC. 2002 Bacterial chromosome extraction and isolation. *Lab Chip* **2**, 207–212. (doi:10.1039/B208010A)
13. Cao H, Yu ZN, Wang J, Tegenfeldt JO, Austin RH, Chen E, Wu W, Chou SY. 2002 Fabrication of 10 nm enclosed nanofluidic channels. *Appl. Phys. Lett.* **81**, 174–176. (doi:10.1063/1.1489102)
14. Riehn R, Lu MC, Wang YM, Lim SF, Cox EC, Austin RH. 2005 Restriction mapping in nanofluidic

Downloaded from http://rsfs.royalsocietypublishing.org/ on December 31, 2014

devices. *Proc. Natl Acad. Sci. USA* **102**, 10 012–10 016. (doi:10.1013/pnas.0503809102)

15. Reisner W *et al*. 2005 Statics and dynamics of single DNA molecules confined in nanochannels. *Phys. Rev. Lett.* **94**, 196101. (doi:10.1103/PhysRevLett.94.196101)
16. Duke TAJ, Austin RH, Cox EC, Chan SS. 1996 Pulsed-field electrophoresis in microlithographic arrays. *Electrophoresis* **17**, 1075–1079. (doi:10.1002/elps.1150170616)
17. Huang LR, Tegenfeldt JO, Kraeft JJ, Sturm JC, Austin RH, Cox EC. 2002 A DNA prism for high-speed continuous fractionation of large DNA molecules. *Nat. Biotechnol.* **20**, 1048–1051. (doi:10.1038/nbt733)
18. Ajdari A, Prost J. 1992 Drift induced by a spatially periodic potential of low symmetry-pulsed dielectrophoresis. *CR Acad. Sci. Ser. II* **315**, 1635–1639.
19. Duke TAJ, Austin RH. 1998 Microfabricated sieve for the continuous sorting of macromolecules. *Phys. Rev. Lett.* **80**, 1552–1555. (doi:10.1103/PhysRevLett.80.1552)
20. Rousselet J, Salome L, Ajdari A, Prost J. 1994 Directional motion of Brownian particles induced by a periodic asymmetric potential. *Nature* **370**, 446–447. (doi:10.1038/370446a0)
21. Austin RH, Darnton N, Huang R, Sturm J, Bakajin O, Duke T. 2002 Ratchets: the problems with boundary conditions in insulating fluids. *Appl. Phys. A Mater. Sci. Process.* **75**, 279–284. (doi:10.1007/s003390201336)
22. Huang LR, Cox EC, Austin RH, Sturm JC. 2004 Continuous particle separation through deterministic lateral displacement. *Science* **304**, 987–990. (doi:10.1126/science.1094567)
23. Purcell EM. 1977 Life at low Reynolds number. *Am. J. Phys.* **45**, 3–11. (doi:10.1119/1.10903)
24. Loutherback K, Puchalla J, Austin RH, Sturm JC. 2009 Deterministic microfluidic ratchet. *Phys. Rev. Lett.* **102**, 045301. (doi:10.1103/PhysRevLett.102.045301)
25. Millner LM, Linder MW, Valdes R. 2013 Circulating tumor cells: a review of present methods and the need to identify heterogeneous phenotypes. *Ann. Clin. Lab. Sci.* **43**, 295–304.
26. Comen EA. 2012 Tracking the seed and tending the soil: evolving concepts in metastatic breast cancer. *Discov. Med.* **14**, 97–104.
27. Lee Y, El Andaloussi S, Wood MJA. 2012 Exosomes and microvesicles: extracellular vesicles for genetic information transfer and gene therapy. *Hum. Mol. Genet.* **21**, R125–R134. (doi:10.1093/hmg/dds317)
28. Moon PG, You S, Lee JE, Hwang D, Baek MC. 2011 Urinary exosomes and proteomics. *Mass Spectrom. Rev.* **30**, 1185–1202. (doi:10.1002/mas.20319)